Vol. 277: 37–50, 2004 | MARINE ECOLOGY PROGRESS SERIES
Mar Ecol Prog Ser | Published August 16

Phytoplankton productivity on the Canadian Shelf of the Beaufort Sea

Eddy C. Carmack[1,*], Robie W. Macdonald[1], Steve Jasper[2]

[1]Institute of Ocean Sciences, 9860 West Saanich Road, Sidney, British Columbia, V8L 4B2, Canada
[2]Essjay Ventures Inc., 72 Beech St., Comox, British Columbia, V9M 3W7, Canada

ABSTRACT: For the first time, the seasonal cycle of phytoplankton productivity on a broad, seasonally ice-covered arctic shelf (the Canadian Shelf of the Beaufort Sea) is examined. This shelf is the most riverine of the panarctic shelves. During 5 surveys between April and September 1987, field observations (salinity, temperature, nutrients, photosynthetically active radiation [PAR], chlorophyll *a*) and shore-based data (air temperature, river discharge, sea-ice cover, PAR) were collected. Productivity was measured using ^{14}C and converted to daily production with PAR and vertical light extinction values. Due to inflow from the Mackenzie River, phosphorus limits production over the inner shelf (depth $z < 20$ m) whereas nitrogen limits production over the middle ($20 < z < 80$ m) and outer (shelf-break; $z > 80$ m) shelf. Light limitation due to landfast ice delays the onset of water-column productivity in spring in the inner shelf by about 1 mo compared to the outer shelf. In spring, maximum productivity occurred near the surface and decreased exponentially with depth. In summer, as nutrients became depleted in the upper mixed layer, a deep chlorophyll maximum developed toward the bottom of the winter mixed layer (20 to 40 m). Productivity during spring (ice cover) was about 10 mg C m^{-2} d^{-1}, rising typically to about 200 mg C m^{-2} d^{-1} by late July. Maximum productivities, ~600 mg C m^{-2} d^{-1}, were observed above the head of Kugmallit Canyon, suggesting enhanced upwelling. The total production for 1987 was estimated at 12 to 16 g C m^{-2}, characteristic of oligotrophic waters. This range is consistent with new-production estimates based on nutrient draw-down over the shelf and on vertical carbon fluxes at the shelf break measured by sequential traps or ^{234}Th disequilibria. Light limitation due to snow and ice cover may control the timing of primary production, but the availability of nutrients ultimately sets the annual limit. Nutrient availability is determined partly by cumulative vertical convection during winter, and partly by upwelling. Projected loss of ice cover over the Arctic's marginal seas is likely to have its greatest impact by widespread initiation of conditions for shelf-break upwelling.

KEY WORDS: Arctic · Nutrients · Primary production · Shelf

INTRODUCTION

By their size alone, the large continental shelves that comprise over 50% of the surface area of the Arctic Ocean play a key role in producing food, sequestering organic carbon and establishing property distributions within the arctic basin (cf. Macdonald et al. 1998, Aagaard et al. 1999, Carmack & Macdonald 2002). For a great part of the year arctic shelves are covered by sea ice, and such seasonality significantly affects hydrographic conditions and primary productivity. The presence and timing of sea-ice cover controls the availability of solar irradiance, limits the development of stratification by heating and freshwater input, and shields the underlying water column from wind-driven vertical mixing and shelf-break upwelling. The need to understand the joint roles of these various environmental factors is made all the more urgent if we are to predict changes in the productivity of the Arctic Ocean under scenarios of climate variability. In the present

*Email: carmacke@pac.dfo-mfo.gc.ca

study we describe the first seasonality study of the annual cycle of phytoplankton productivity, carried out on the Canadian Shelf in 1987, with emphasis on the role and timing of environmental forcing parameters.

The Canadian Shelf (Fig. 1) in the southeastern Beaufort Sea is a broad rectangular shelf (width ~120 km; length ~530 km) that is bordered by the Amundsen Gulf to the east, Mackenzie Canyon to the west, the Mackenzie River delta to the south and the Canada Basin to the north (shelf-break ~80 m depth). Two submarine canyons cross the shelf: the broad, deep Mackenzie Canyon at about 138° W, and the narrow, relatively shallow Kugmallit Canyon at about 134° W. This shelf is the most 'riverine' of pan-arctic shelves receiving annually a freshwater burden (330 km^3) which, if spread over the shelf (60 000 km^2), would exceed 6 m (Macdonald et al. 1989). As such, the shelf behaves as an estuarine system that derives its water and associated material properties from both oceanic and terrestrial sources (Carmack et al. 1989, Macdonald et al. 1989). The origin of water drawn onto the shelf from the adjacent ocean is significant both as a source of nutrients and as a source of seed biological populations. The key point here is that the upper (0 to 220 m) waters of the adjacent Canada Basin are mainly supplied by relatively nutrient-rich Pacific Ocean inflows through Bering Strait, which arrive off the shelf-break of the Canadian Shelf as both summer (Bering Sea Summer Water, BSSW, S ~32.4) and winter (Bering Sea Winter Water, BSWW, S ~33.1) water mass varieties (Coachman & Barnes 1961, Macdonald et al. 1989, Shimada et al. 2001). Deeper waters offshore (below ~220 m) originate in the Atlantic Ocean and Nordic Seas (McLaughlin et al. 1996, 2002). Because the shelf break on the Canadian Shelf lies at ~80 m, upwelling events mainly move waters of Pacific origin onto the shelf; limited observations suggest shelf-basin exchange is enhanced by upwelling in both Kugmallit and Mackenzie Canyons (Macdonald et al. 1987, Carmack & Kulikov 1998, for extreme events). The presence of the Mackenzie River likewise insures inputs of freshwater biota and land-derived nutrients, especially in the upper 5 to 10 m of the coastal ocean. Our partitioning of the shelf is based partly on the distribution of ice and Mackenzie River water as discussed by Macdonald et al. (1995) and partly on the processes affecting water distribution (winds, river inflow and sea-ice cover variability) as discussed and modelled by Omstedt et al. (1994).

Little work has been published on phytoplankton productivity on interior Arctic shelves in general and the mainland Canadian Shelf in particular (cf. Sakshaug 2003). Several studies have examined the relative contributions from ice and pelagic algae to total productivity in the Alaskan Beaufort region (Alexander 1974, Horner 1981, Horner & Schrader 1982), and noted that while ice algae constitute only about 10 to 15% of the total annual production, they are an important food source early in the growing season. Grainger (1975) and Hsiao (1996) made measurements in summer (open water) over the Canadian Shelf and identified diatoms and flagellates as important contributors to production, with diatoms being more important in the nearshore region. Macdonald et al. (1987) estimated new produc-

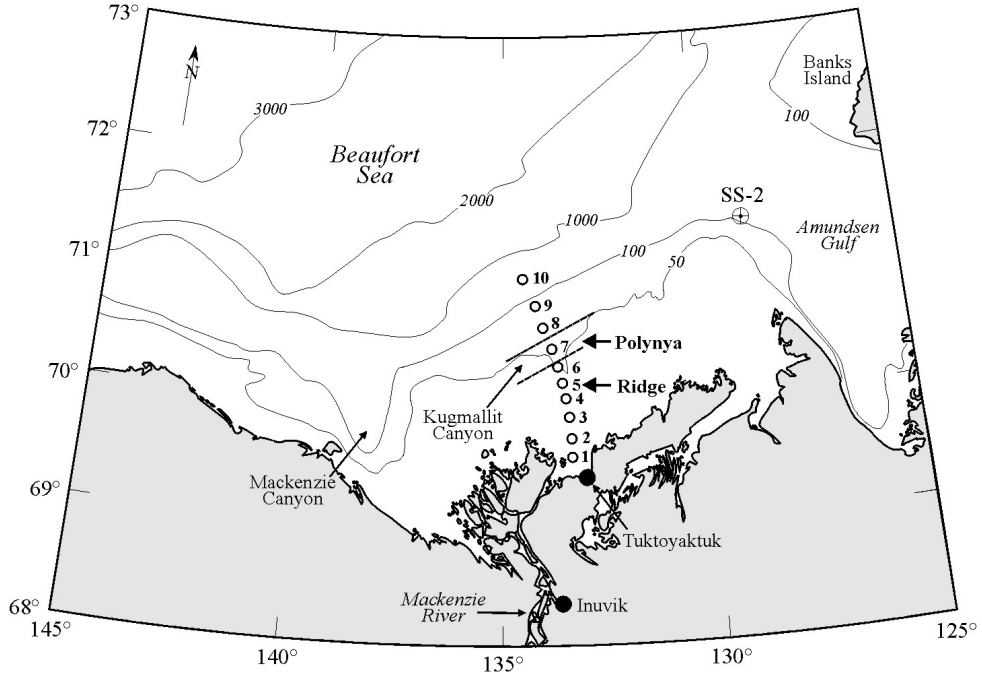

Fig. 1. Study area and location of Line C stations (1 to 10), the PAR measurement site in Tuktoyaktuk and the moored sediment trap at SS-2

tivity on the Canadian Shelf from nutrient uptake relationships; they compared a heavy ice year (1974) with a light ice year (1975) and found a reduction in new productivity of about 30% (16 and 23 g C m^{-2} yr^{-1}, respectively). Parsons et al. (1988, 1989) reported on phytoplankton and zooplankton distributions in summer, noting significant regional differences in biological parameters. Specifically, 2 distinct communities were found: a heterotrophic riverine community characterized by high dissolved organic carbon, bacterial activity and gammarid amphipods, and a more productive, autotrophic offshore community characterized by phytoplankton, marine zooplankton and jellyfish.

In this paper we present data collected during 5 time intervals spanning early spring to late summer in order to discuss the joint roles of ice cover and nutrient availability in determining the seasonal cycle of primary pelagic productivity on a broad, riverine arctic shelf. The 5 time intervals span the period leading up to the onset of under-ice production in spring through to the end of open-water, summer production. These 5 time periods are augmented by continuous measurements of shore-based photosynthetically active radiation (PAR) and sediment trap measurements; limitations to the data coverage, particularly in early summer, are discussed below. Given the mechanisms that presently control the timing and quantity of primary production, we speculate how projected change is most likely to alter arctic shelf productivity.

MATERIALS AND METHODS

Environmental data. Oceanographic measurements were obtained during 5 surveys between early April and early September 1987, at 10 stations along a section (referred to as Line C) immediately north of the Mackenzie River (Fig. 1, Table 1). The sampling interval terminated before freeze-up (usually mid-October) allowing the possibility of missing production during fall blooms. However, at this time low light levels and mixed-layer deepening likely constrain the potential for substantial fall productivity. During the ice-covered sampling period (early April to June) stations were accessed by helicopter and fixed-wing aircraft; in summer stations were reached aboard the CSS 'J.P. Tully'. For aircraft-based surveys a self-contained Applied Microsystems CTD was used to measure temperature and salinity; accuracies are estimated to be T = ±0.02°C and S = ±0.04. For shipboard measurements a Guildline CTD was used; accuracies are estimated to be T = ±0.01°C and S = ±0.01. Nutrients (nitrate, silicate and phosphate) were obtained using 1.7 (ice work) and 5 l (ship work) Niskin bottles and analyzed by standard methods using a Technicon Autoanalyser. During spring ice work, samples were frozen and returned to the Institute of Ocean Sciences (IOS) to be analyzed. Where there was visible turbidity, samples were filtered through a Millipore 0.45 µm HA filter, washed with Milli-Q deionized water, before subsampling into tubes and freezing. Methods of nutrient analysis and precisions based on duplicate analyses are given in Macdonald et al. (1988a,b).

Water samples for incubation were likewise collected in Niskin bottles and subsampled into translucent or opaque bottles. These were kept cool and incubated within 3 h of collection. Water samples were screened through 110 µm Nitex mesh to remove large grazers, and aliquots were then removed for chlorophyll *a* and photosynthesis-irradiance ratio (P-I) determinations. Chlorophyll *a* was determined by 1 l filtration through 0.45 µm glass fiber filters, extraction into 90% acetone solution using a Polytron homogenizer, and subsequent photometric analysis at 665 nm before and after acidification to correct for pheopigments (Lorenzen 1967). At each biological measurement station, profiles were made of the extinction of photosynthetically available radiation (PAR) using a Licor underwater quantum sensor. Continuous measurements of PAR were also taken using a Licor atmospheric quantum sensor located at the Polar Continental Shelf base in Tuktoyaktuk. Supplemental

Table 1. Stations, water depths and survey dates (dd/mm) for stations occupied for phytoplankton productivity measurements on the Canadian Shelf in 1987

		Stn no.						
		1	3	4	5	7	9	10
Latitude (N)		69° 32.5′	69° 47.1′	69° 53.5′	70° 01.0′	70° 15.8′	70° 44.2′	70° 56.8′
Longitude (W)		133° 17.5′	133° 21.0′	133° 24.7′	133° 26.0′	133° 39.2′	134° 09.9′	134° 35.7′
Depth (m)		3	10	15	25	50	60	200
Survey no.	1	11/04		09/04	07/04		03/04	
	2	05/05		28/04		23/04		
	3			29/05	26/05		24/05	23/05
	4		01/08	02/08	03/08	06/08	05/08	04/08
	5				04/09	03/09	02/09	

environmental data on air temperature, Mackenzie River streamflow and sea-ice cover were obtained from databases supported by Environment Canada.

Incubation procedure and estimation of daily production. Primary production was not measured but calculated based on P-I curves. Two incubators were used to determine photosynthetic light curves (for methodology see Jasper et al. 1983, Jasper & Bothwell 1986). Each consisted of a plexiglass tank (1.07 m × 0.61 m × 0.30 m) separated into 6 compartments, each holding up to twelve 250 ml clear plastic bottles, and illuminated from below with irradiance determined by a combination of neutral density plexiglass and plastic screens. Varying the number of layers of plastic screens in each compartment provided 6 levels of irradiance in the incubator. The irradiance levels were neutral-density filters adjusted to mimic light levels observed in vertical profiles at sampling stations during each season. Layers of UV-absorbing plexiglass (UF1, Rhom and Hass) and blue plexiglass (#2069, Rohm and Haas) were placed between the light source and the tank. The blue plexiglass simulates the spectral composition of light at 5 m depth in coastal waters (Harrison et al. 1977). The light source during the spring (April to May) measurements consisted of twelve 40 W daylight fluorescent lamps and during the summer (August to September) period two 400 W metal halide lamps. Each compartment had a specific irradiance level determined by a combination of neutral density plexiglass screens adjusted to best match the P-I curve at a particular time of the growing season. Typically, incubation times were between 4 and 6 h, and incubator temperatures were kept near ambient surface water temperatures.

Fig. 2 provides a schematic illustration of the procedure for calculating production in the water column based on ^{14}C uptake and observed light and chlorophyll *a* profiles (see Jasper et al. 1983, for details). First, the surface PAR value was obtained from the shore-based continuous (10 min interval) record (Fig. 2a). Second, the underwater light profile collected on a given sampling day was linearly interpolated for dates between sampling days using the continuous light records (Fig. 2b), and for every day, profiles of chlorophyll *a* (chl *a*) and P-I were linearly interpolated between sampling days. Third, for each depth interval within the euphotic zone, the fraction of available light was obtained either by measurement or interpolation. Fourth, from the P-I curves determined by incubation, the values of chlorophyll production ($P[chl\ a]^{-1}$) were calculated using the *in situ* irradiance. Finally, the value $P[chl\ a]^{-1}$ (Fig. 2c) was multiplied by the chl *a* value (Fig. 2d), either measured or interpolated, at that given depth. This procedure was repeated for all time intervals between cruise dates for the euphotic zone.

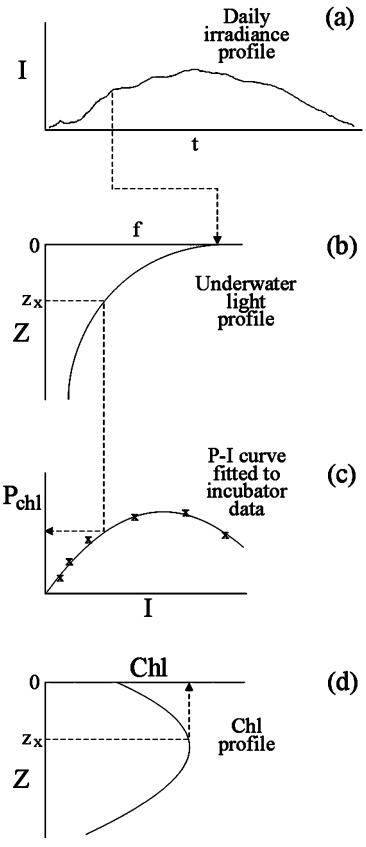

Fig. 2. ^{14}C-incubator methodology. The (a) irradiance on a given day is matched to the (b) observed light extinction profile; the irradiance profile is then combined with the (c) P-I curve fitted to incubator data and the (d) observed chl *a* profile to compute primary productivity. Abbreviations refer to: I = irradiance; t = time; f = fraction of surface irradiance; Z = depth; P_{chl} = productivity

Calculations were carried out following the numerical procedures given by Fee (1969).

RESULTS & DISCUSSION

Oceanographic domains in winter and summer

Schematic sections of oceanographic structure across the Canadian Shelf based on hydrographic data for winter and summer are shown in Fig. 3 (cf. Carmack & Macdonald 2002). Following this conceptual model, it is practical to discuss physical and biological processes in terms of inner shelf (z < ~20 m; Stns 1 to 4), middle shelf (~20 < z < ~80 m; Stns 5 to 8) and outer shelf and shelf-break (z > ~80 m; Stns 9 to 10).

Late winter and the beginning of oceanographic spring, approximately in April, corresponds to the time when sea-ice reaches its maximum thickness (~2 m).

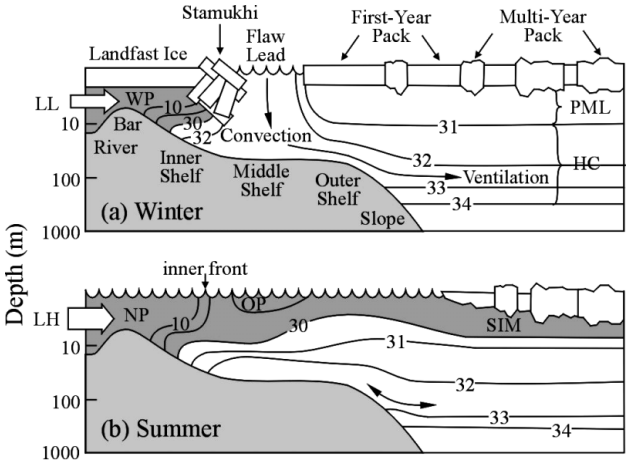

Fig. 3. The water mass structure across the Canadian Shelf in (a) winter and (b) summer; selected isolines of salinity are drawn from Line C data in 1987. Abbreviations: LL = lower low river discharge; LH = lower high river discharge; WP = winter plume; NP = new (summer) plume; OP = old (winter) plume; PML = polar mixed layer; HC = halocline complex; SIM = sea ice melt

At this time, the relatively flat landfast ice extends seaward from the coast to approximately the 20 m isobath. The stamukhi, a field of rubble ice formed by convergence of landfast and drifting ice, forms the outer boundary of landfast ice. The Mackenzie River inflow in winter, while relatively low (~4000 $m^3 s^{-1}$) compared to that of summer (30 000 $m^3 s^{-1}$) still delivers substantial quantities of fresh water to the ocean, where it is largely trapped as a 'floating freshwater lake' (Lake Herlinveaux) in the inner shelf domain behind the stamukhi dam (Macdonald & Carmack 1991, Macdonald et al. 1995, Carmack & Macdonald 2002). The landfast ice and stamukhi thus define a unique inner shelf 'environment' in winter. The shear zone at the boundary of landfast and pack is extremely dynamic, is subject to the rapid opening of a long (over 100 km) and wide (up to 40 km in 1987) 'flaw' polynya running parallel to the coast, and is highly variable from year to year. Sea-ice conditions beyond the flaw polynya are markedly different from the inner shelf, consisting of a complex mixture of heavily ridged and drifting first-year and multi-year pack ice. The outer shelf is recognized as a domain subject to shelf-break dynamics and shelf/basin exchange processes.

Nutrient concentrations in the surface layers at the end of winter are set by the degree of vertical mixing and entrainment that occurred during the preceding fall and winter. The transition to summer begins in late April and early May with the break-up of river ice in the headwaters of the Mackenzie River and the subsequent flooding of the delta and coastal area. According to Dean et al. (1994), heat from the Mackenzie River, which overflows and underflows the landfast ice in the nearshore, accelerates ice removal in the nearshore delta region. Break-up of the middle and outer shelf typically spreads from existing open water in the flaw polynya, where incoming solar radiation is more rapidly absorbed by the water. During break-up, the landfast ice and much of the existing pack ice melts in place. This addition of buoyant, fresh water is mixed downwards by the wind to form a shallow, relatively fresh, mixed-layer of ~10 to 12 m depth, thus stratifying the upper ocean. At the same time, large amounts of fresh and highly turbid water are delivered by the Mackenzie River. Such water is distinct from sea-ice melt and is often observed to form extensive plumes of turbid water, of ~5 m typical thickness, extending across and, at times, off the shelf (Macdonald et al. 1989, 1999), greatly supplementing surface stratification from ice melt. In the absence of winds or under westerly (downwelling favourable) winds, the incoming river water will tend to bend eastward along Tuktoyaktuk Peninsula towards Amundsen Gulf (see Giovando & Herlinveaux 1981). Easterly (upwelling favorable) winds will draw deeper (Pacific-origin) waters onshore and drive plume waters offshore.

It is important to account for vertical as well as horizontal structures in water masses of the Canadian Shelf. The temperature and salinity vertical profiles from summer data (Fig. 4) illustrate the multiple, step-like halocline structures extant in the Beaufort Sea. The salinity structure (which dominates the density stratification) progresses downwards as a series of modes (low-gradient layers) and clines (high-gradient layers) according to the origin of the individual layers. Sequentially, in Fig. 4, these are the upper mixed layer (S < ~31.6), the BSSW halocline (S ~ 32.4) and the BSWW mode water (S ~ 33.1). Waters below BSWW

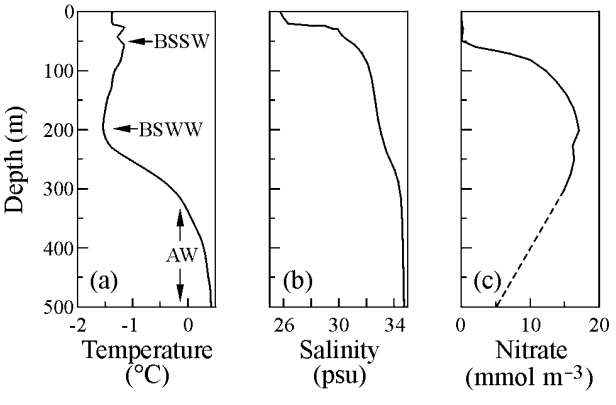

Fig. 4. (a) Temperature, (b) salinity and (c) nitrate profiles showing hydrographic structure in the Canada Basin adjacent to the Canadian Shelf during summer. Abbreviations: BSSW = Bering Sea Summer Water; BSWW = Bering Sea Winter Water; AW = Atlantic Water

are predominately of Atlantic origin and are discussed by McLaughlin et al. 2002. It is also important to note that interannual variability in sea-ice extent and predominant wind direction may result in significant variability in hydrographic structure and biological productivity, so that any given year, including 1987, should not necessarily be taken as 'typical' of seasonal conditions.

Environmental forcing parameters

The background physical environment for air temperature, river discharge and solar irradiance is shown in Fig. 5. Air temperatures (Fig. 5a) play a critical biological role by regulating (a) the melting of snow cover within the watershed and initiating spring runoff, (b) the melting of snow on sea ice and associated changes in albedo, and (c) the timing of sea-ice break-up; all key factors in determining the underwater light climate. During the growing season air temperatures vary over a range of almost 60°C; they fluctuate widely (ca. −40 to 0°C) in April and May with the passage of synoptic weather systems, typically rise above 0°C in early June, and then drop below 0°C in early October, signalling the onset of freeze-up. October and November are also months of strong winds and the passage of polar lows (data not shown), which serve to mix the water column and force shelf/basin exchange. The timing and magnitude of Mackenzie River discharge (Fig. 5b) influences phytoplankton productivity directly through the seasonal delivery of nutrients, sediments and plankton, and indirectly through a regulation of vertical and horizontal density gradients, and shading by turbidity which strongly affects underwater light climate. The time history of PAR (Fig. 5c) illustrates another important feature of Arctic pelagic systems: namely that even though PAR levels are relatively high by early April, this irradiance is mainly reflected upwards by the high albedo of snow and sea ice. Owing to the length of days during the Arctic growing season, the absolute values of daily-integrated PAR equal those typical of temperate latitudes.

The time series of sea-ice cover averaged over the width of the Canadian Shelf (see Fig. 6 for 1987) is an especially critical factor owing to its effect on underwater light and wind forcing, and the PAR time series (cf. Fig. 5c) must be interpreted with respect to snow

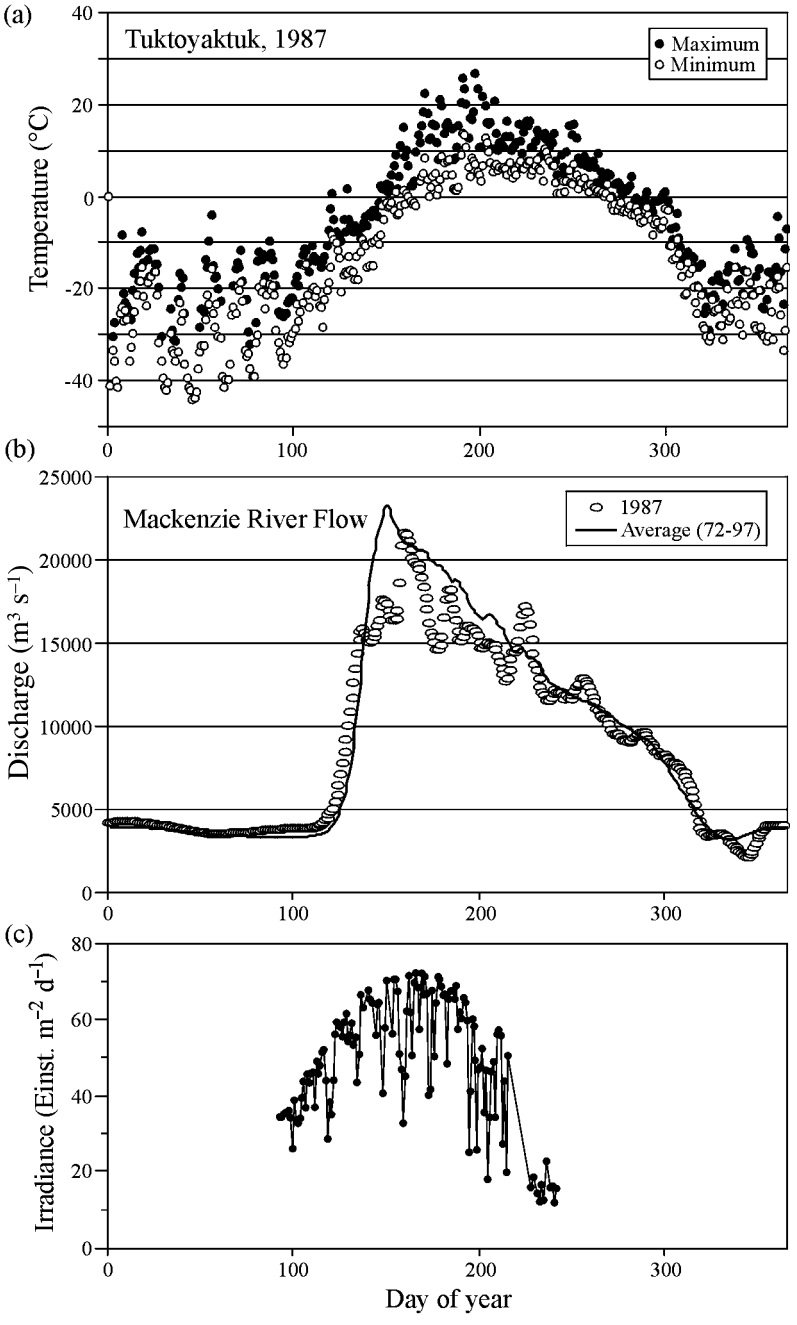

Fig. 5. (a) Air temperature, (b) Mackenzie River discharge and (c) PAR for 1987. Air temperatures were obtained from the Environment Canada station in Inuvik. Mackenzie River streamflows were obtained from the Water Survey of Canada. PAR was recorded at the Polar Continental Shelf Project base in Tuktoyaktuk

and ice cover. The historical record of sea-ice cover from 1968 to 2000 (not shown, but see Carmack & Chapman 2003), available from the Canadian Ice Centre of Environment Canada, shows that 1987 was a moderately light ice year, in that the seasonal ice zone retreated a significant distance off shore, thus allowing exposure of shelf waters to solar radiation and wind forcing. Break-up began in early June in the mid-shelf domain immediately seaward of the landfast ice and stamukhi, and was followed in early July by the rapid deterioration of the landfast ice. By mid-July, sea-ice over the entire Canadian Shelf was reduced to less than one-tenth cover. The outer boundary of sea-ice moved in and out above the continental slope intermittently over the course of summer, in response to synoptic wind events. In early September, for example, onshore (downwelling favourable) winds drove loose pack-ice back onto the shelf, briefly bringing the concentrations above one-tenth in the outer shelf domain. Freeze-up began in mid-October and progressed seaward with the formation of landfast ice and shoreward as the pack-ice froze southward. Complete ice-cover was established in early November.

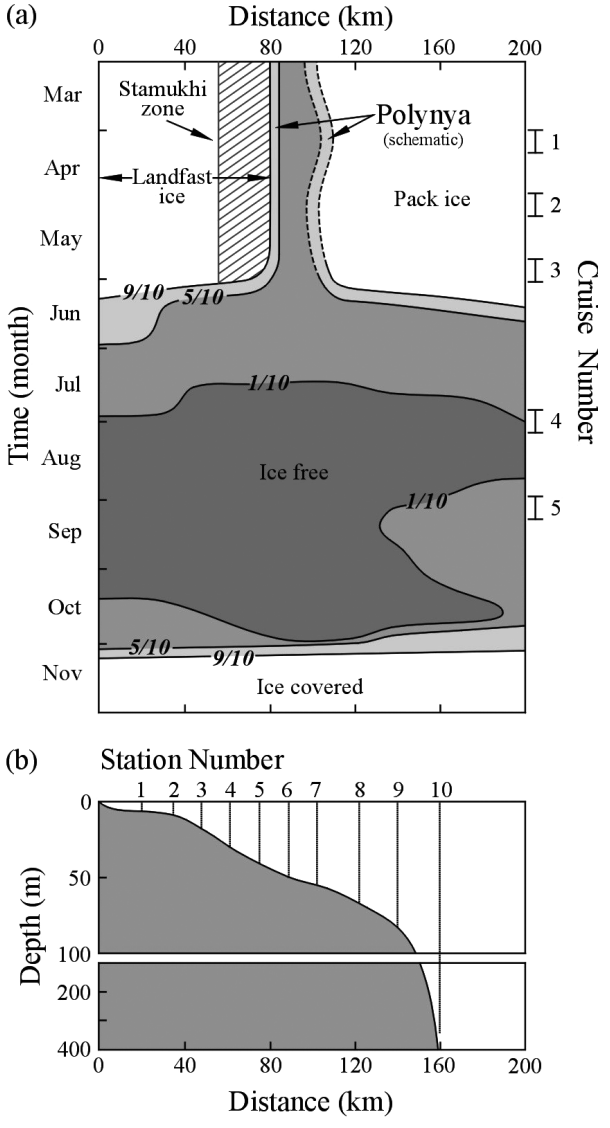

Fig. 6. (a) Sea-ice cover on the Canadian Shelf for the period April to November 1987, based on data obtained from the Canadian Ice Centre, Environment Canada; approximate dates of the 5 sampling periods are shown on the right axis. (b) The cross-section of the Canadian Shelf near Line C and the location of sampling stations

Underwater light conditions dictate the timing of the onset and end of phytoplankton productivity. For example, in April the surface layer nutrients (Fig. 7) and solar irradiance (Fig. 5c) are sufficient to initiate growth, but the onset of pelagic productivity is delayed. In the landfast ice domain, the water is shaded by both ice and snow cover, and algal production is likely limited to the bottom fraction of the sea-ice (cf. Horner & Schrader 1982). In the flaw polynya domain, brine-driven deep convection prohibits a stable light climate for phytoplankton growth. Farther offshore, in the pack-ice domain, snow and ice cover again limit light and delay the onset of productivity. In the fall, the daylight rapidly diminishes from 12 h at the equinox (September 21) to total darkness by mid November, and low sun angle further limits light penetration.

Nutrient distributions

Correlation diagrams of nitrate, phosphate and silicate versus salinity for late winter (April to May) and summer (September) 1987 (Fig. 7) show both spatial and seasonal variability. During winter (Fig. 7a–c), nutrients in the inner shelf are dominated by inputs from the Mackenzie River. At this time nitrate and silicate values in the inner shelf are relatively high, 4 to 9 mmol m^{-3} and 40 to 60 mmol m^{-3}, respectively. Phosphate levels, however, are very low, ranging from near zero to 0.2 mmol m^{-3} in waters of salinity S ~ 20, a condition characteristic of inland waters. There are 2 noteworthy points concerning winter nutrient distributions. First, the zero intercept for phosphate is at a salinity of about 5, suggesting that there are abiotic removal processes—probably associated with iron flocculation—within the near-shore estuary, and this strongly suggests that phosphate is the limiting nutrient for primary productivity in the inner shelf domain (see Macdonald et al. 1987). Second, the silicate mixing line during winter (Fig. 7c) branches at a salinity of ~31 and silicate ~20 mmol m^{-3}: points trending upwards to the left toward >60 mmol m^{-3} silicate identify the inner shelf domain influenced by river water; whereas points trending downward to the left toward

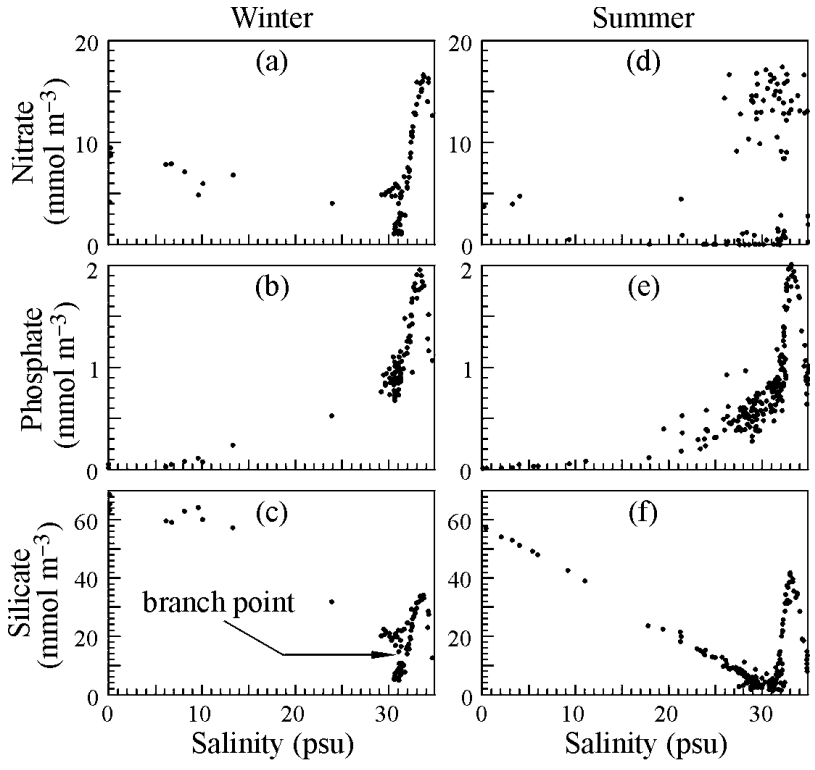

Fig. 7. Correlation diagrams of salinity versus nitrate, phosphate and silicate across the Canadian Shelf along Line C in (a–c) April 1987 and (d–f) September 1987

low silicate values identify outer-shelf surface waters that remain silicate depleted. This bifurcation is further evidence of separation between inner and middle-to-outer shelf and that vertical convection in the middle-to-outer shelf has not penetrated deeply enough to access nutrient-rich water (BSWW).

All nutrients in the wintertime data (Fig. 7a–c) show a pronounced break-point in the mixing lines at salinities near 31.6, the core salinity of the winter mixed layer (cf. Carmack et al. 1989). Both nitrate (~1 to 2 mmol m^{-3}) and silicate (~2 to 3 mmol m^{-3}) show clear minima at this point, while phosphate shows an inflection point. All nutrients then increase with increasing salinity to the core of BSWW, with nitrate reaching ~15 mmol m^{-3}, phosphate reaching ~2 mmol m^{-3} and silicate reaching ~30 mmol m^{-3} at salinities near 33.1 (Macdonald et al. 1989). This illustrates a key point. The winter mixed-layer of the Canadian Shelf overlies the nutrient-rich waters of Pacific origin but, based on the nutrient-salinity relationship shown in Fig. 7a–c, winter convection driven by brine formation does not efficiently tap these deeper nutrients. Rather, we see a mixing line that incorporates a Mackenzie River end member (10 mmol m^{-3} nitrate, 0 mmol m^{-3} phosphate and 65 mmol m^{-3} silicate) and a 'bottom of the mixed layer' end member (~5 mmol m^{-3} nitrate, ~0.7 mmol m^{-3} phosphate, ~20 mmol m^{-3} silicate). The access to the deeper, Pacific nutrients is restricted partly because the inventory of freshwater runoff from the Mackenzie River remaining in winter is not fully compensated by fall and winter salinification by ice formation or shelf-edge exchange (Macdonald 2000), and partly because when brine of sufficient density is formed, it sinks and advects across the shelf as a near-bottom plume, thus removing regenerated nutrients from the shelf (see Melling & Lewis 1982). As a consequence, surface-layer nutrient values from winter (e.g. 3 to 10 mmol m^{-3} nitrate, Fig. 7a), which are supplied by river inflow and water from the top of the nutricline (Fig. 4c), severely constrain productivity in spring and summer. New productivity beyond the pre-conditioned wintertime set-up would then require shelf-break and canyon upwelling and/or turbulent fluxes, e.g. by tidal or wind mixing through the S = 31.6 halocline into the euphotic zone. The main impact of sea-ice cover on seasonal productivity, be it new production or recycled production, is not so much in limiting light, but more in determining the efficiency of wind mixing and shelf-break exchange in a system that is essentially nutrient-limited.

Nutrient distributions in summer (Fig. 7d–f) reveal a complex pattern of nutrient uptake across the shelf. In the inner shelf (e.g. within the Mackenzie plume) phosphate values remain near zero, while nitrate values remain relatively high; again, a distribution characteristic of phosphorus-limited inland waters (cf. Grainger 1975). Silicate values form an apparent mixing line between Mackenzie River source water at S = 0 and the BSSW halocline at S = 31.6. There are 2 important differences between the winter (Fig. 7c) and summer (Fig. 7f) silicate-salinity distributions. First, the branch point described above for winter is missing in summer. Second, the summer mixing line is offset ~20 mmol m^{-3} lower in silicate than the winter line, suggesting silicate uptake by diatoms in the inner shelf domain (Parsons et al. 1988, Hsiao 1996). In the middle and outer shelf, silicate values remain low in summer and thus suggest favoring of smaller phytoplankton, such as flagellates, over larger phytoplankton such as diatoms (cf. Hsiao 1996). In the middle shelf, at salinities between 26 and 30, nitrate values are bimodal, being either near-zero or relatively high (above 10 mmol m^{-3}). This suggests that beyond the plume transition zone (inner shelf) the primary produc-

tivity is either nutrient limited (as in clear or ice-free water) or light limited (as in turbid or ice-covered water). Silicate values in the S = 30 to 32 range are depleted relative to late winter values, suggesting diatom uptake and limitation.

The observed uptake of nutrients between winter and summer allows us to make rough estimates of the new production (NP), in g C m^{-2} yr^{-1} (see Reigstad et al. 2002, for Barents Sea application). The conversion of nutrient data in the ocean to carbon units requires knowledge of the ratio of uptake (the so-called Redfield Ratio), which for C:N is usually assumed to be ~6.6:1 (weight to weight). The depletion of silicate relative to nitrate can indicate whether the main producers are diatoms or non-silicate consuming phytoplankton (e.g. flagellates – see for example Koike et al. 2001). Silicate to nitrate ratios, however, are highly variable, for example 2.14 in the Bering Sea, 2.36 in the Chukchi Sea and 1.87 in the Eastern Canadian Arctic (Codispoti & Richards 1968, Anderson & Dyrssen 1981, Harrison & Cota 1990, Koike et al. 2001). Making the reasonable assumption that the water residence time (~6 to 12 mo Macdonald et al. 1989, Omstedt et al. 1994) exceeds the length of the growing season (~3 to 4 mo), the drawdown of nitrate (~2 mmol m^{-3} to a depth of ~50 m) observed here over the middle and outer Mackenzie Shelf implies a NP of ~8 g C m^{-2} yr^{-1}. This number certainly underestimates the true NP, as it ignores supply by upwelling and loss by advection at the shelf edge. Similarly for silicate, if we take a Si:N ratio of 2.1 to 2.4, as observed in the Bering and Chukchi seas, the silicate drawdown of ~3 mmol m^{-3} over the middle and outer Mackenzie Shelf implies a NP of 5 to 6 g C m^{-2} yr^{-1}. Similar calculations for the inner shelf domain yield NP values of 3 to 12 g C m^{-2} yr^{-1}; such estimates, however, are problematic because the residence time of the shallow, coastal plume is short (<1 mo) compared to the growing season.

Phytoplankton productivity

Our data represent an effort to collect a productivity time-series that spans the spring (ice-covered) and the summer (open-water) periods; however, the data coverage was not uniform (Table 1) due to logistical difficulties (i.e. sampling from aircraft in the flaw lead during winter (Stn 7) or sampling from the CSS 'J.P. Tully' in the shallow nearshore zone in summer). Still, the calculated time series of daily primary productivity (Fig. 8), combined with environmental data on sea-ice cover, stratification and nutrients, imply the following seasonal sequence. During spring (April and part of May) productivity values were extremely low (~10 mg C m^{-2} d^{-1}) due to low *in situ* light levels under sea-ice. As light levels increased due to loss of snow-cover through melting and sea-ice break-up, productivity values increased rapidly, especially at the outer Stns 9 and 10. Calculated values at all stations increased through summer, reaching maximum values of about 200 mg C m^{-2} d^{-1} during open-water conditions at the end of July. In August, as nutrients became depleted in the surface layers, productivities decreased to levels similar to those found in early June (about 100 and 40 mg C m^{-2} d^{-1} at Stns 9 and 10, respectively). Such values are typical of oligotrophic waters. It may be argued that the time gap between Surveys 4 and 5 is too great to allow interpolation of P-I characteristics; that is, a bloom may have occurred such that peak productivities were missed.

Some key differences among stations are apparent in Fig. 8. Early in the year, productivity values at Stns 1 to 5 in the inner shelf domain remain low up until late May, whereas the offshore stations (9 and 10) show that productivity starts to climb by the end of April. This general pattern suggests that light limitation continues for a longer period under the landfast and stamukhi ice. In fall, productivity at Stn 5 is lower than at Stn 9, and is lower at both stations by a factor of 2 or 3 than Stn 7 (the only time Stn 7 was accessible). We note that Stn 7 is located near the head of the Kugmallit Canyon, a potential site of upwelling (Carmack & Macdonald 2002). Parsons et al. (1988) also noted larger-sized zooplankton in the vicinity of Stn 7, a distribution that may be due to increased delivery of nutrients associated with canyon upwelling.

Calculated monthly phytoplankton productivities for each station (Fig. 9) yield values ranging from a low of 0.5 g C m^{-2} in April to around 5 g C m^{-2} in July (excluding Stn 7). Production for the entire measurement period (early April to early September) is about 12 g C m^{-2} at Stn 5 and 15 g C m^{-2} at Stn 9. This value, when compared with NP estimated above using nitrate drawdown, yields an f-ratio of 0.67. The high f-ratio implies that most of the nitrogen uptake in the euphotic zone has been in the form of nitrate with little recycling. This suggests, perhaps, that much of the organic matter sinks to the bottom of the shelf during the growing season, a situation that is often characteristic of systems with mismatching phytoplankton and zooplankton cycles (Wassmann 1998). This value is close to the value of 0.4 to 0.6 typically used to model the carbon cycle in the Arctic Ocean (Walsh 1989).

In summer, nutrients are rapidly drawn from the surface layer, resulting in the formation of a deep chlorophyll maximum at 25 to 30 m depth. For example, profiles of temperature, salinity and chlorophyll *a* at Stn 9 (compare Fig. 4 with Fig. 10) clearly show that this maximum is associated with ambient stratifi-

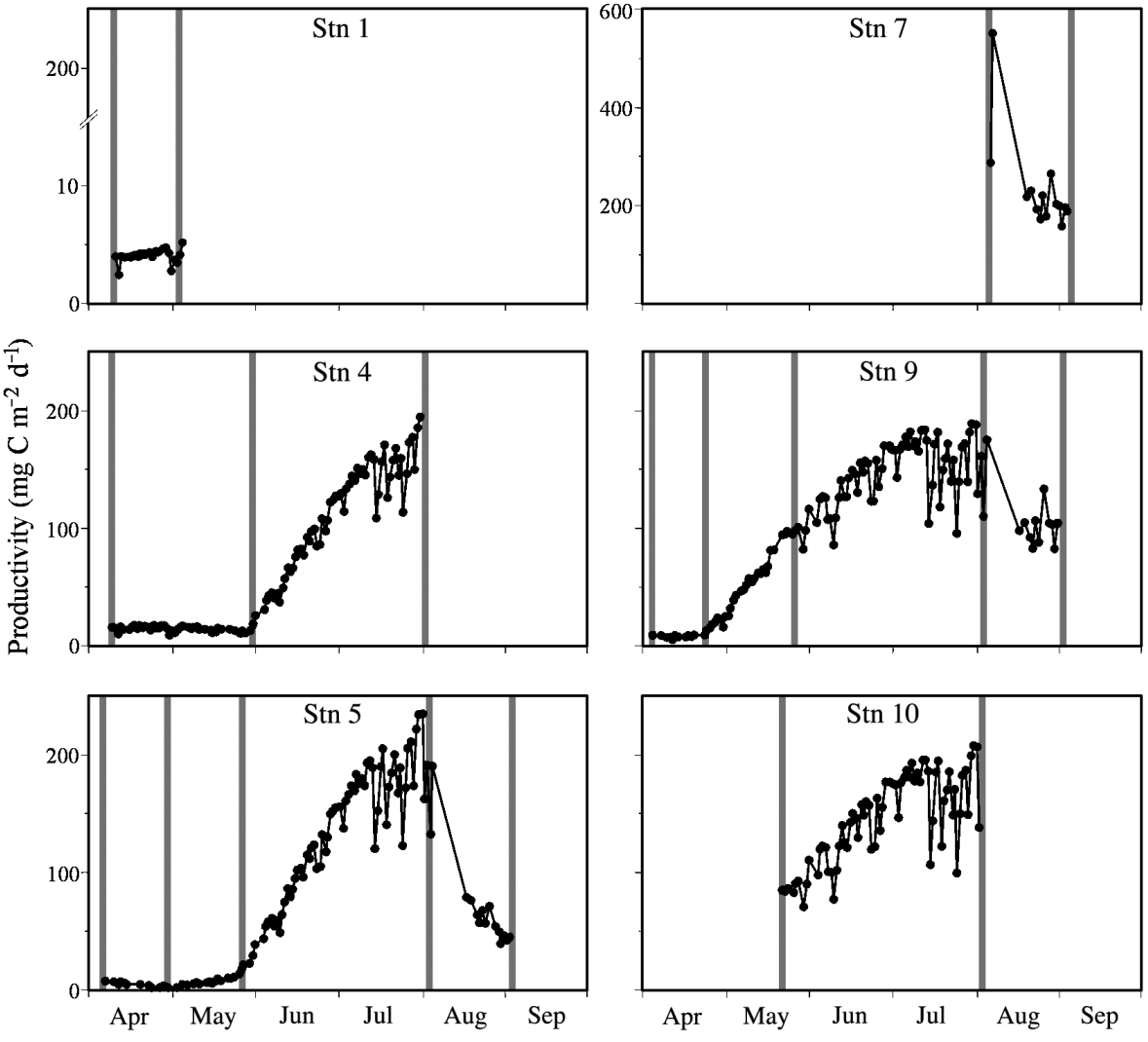

Fig. 8. Calculated daily phytoplankton productivity estimates (mg C m^{-2} d^{-1}) at Line C Stns 1, 4, 5, 7, 9 and 10 for 1987. The vertical gray bands show the spring and summer sampling intervals

cation and the multiple halocline structure extant on the Canadian Shelf. Specifically, a halocline feature at salinities between 31.6 and 32.4 separates the nutrient-poor polar mixed-layer from the underlying nutrient-rich BSSW. The chlorophyll maximum lies at the lower base of this structure. Presumably phytoplankton grow in an environment of relative stability, trading off the availability of PAR and of nutrients. The overall importance of the chlorophyll maximum in sustaining food production on the Beaufort shelf is unknown.

A wider context for the above productivity estimates can be made by examining the carbon flux recorded in a sediment trap between spring 1987 and spring 1988 (O'Brien et al. 1991). This trap, moored at a depth of 150 m off the eastern shelf (SS-2 in Fig. 1), accumulated at least half of its total vertical flux (4.6 g C m^{-2}) after the end of August (Fig. 11). Using a relationship between flux (J) and primary production (PP) previously applied to the Canada Basin (Macdonald & Carmack 1991, J = PP/(0.024z + 0.21), the carbon flux at 150 m implies a surface total PP rate of 17 g C m^{-2} yr^{-1}. During the period of direct productivity measurements (early April to early September), this trap collected approximately 40% of its annual flux of carbon, which would correspond to a total primary production of 7 g C m^{-2} yr^{-1}. In relating sediment trap fluxes to PP measurements we acknowledge the difficulty of establishing error bounds and standard deviations for the 2 kinds of measurement. At face value, the PP estimate (7 g C m^{-2} yr^{-1}) likely represents the 'direct' vertical flux due to PP. The

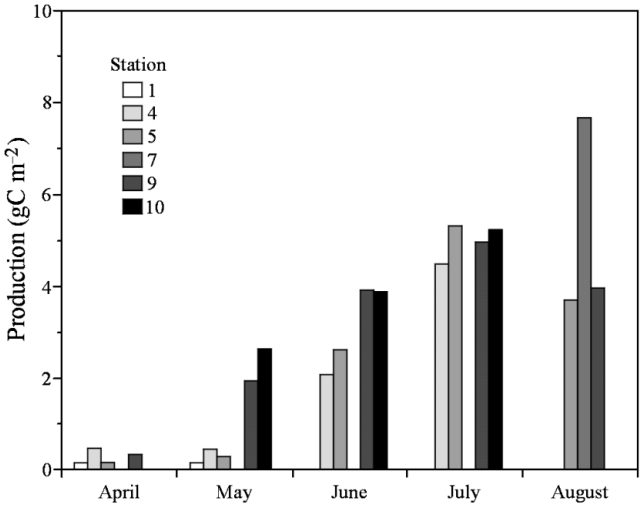

Fig. 9. Monthly phytoplankton productivity at each station

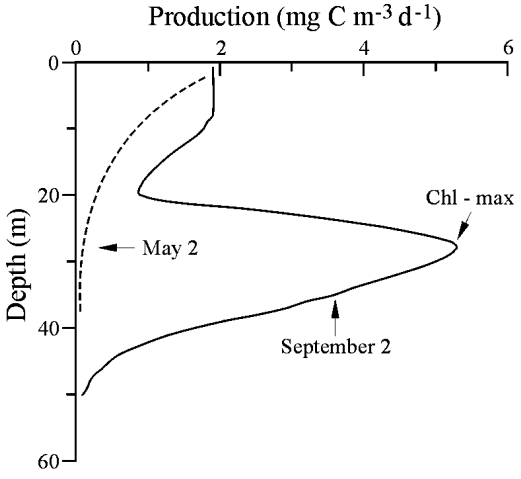

Fig. 10. Profiles of chlorophyll *a* at Stn 9 in May and September 1987

17 g C m^{-2} yr^{-1} captured by the traps could easily be accounted for by resuspension at the shelf-bottom during fall storms followed by advection off the shelf. This latter material could comprise both marine production settled on the shelf bottom plus terrestrial organic carbon delivered to the region by the Mackenzie River and coastal erosion (Macdonald et al. 1998). Finally, using ^{234}Th disequilibria, Moran & Smith (2000) estimated particulate organic carbon (POC) export in the shelf-slope region to be about 4 to 7 mmolC m^{-2} d^{-1} (0.05 to 0.08 g C m^{-2} d^{-1}). These rates, if applied to a 100 d growing season, imply 5 to 8 g C m^{-2} yr^{-1}, again comparable with the other methods of estimation.

Sensitivity of the Beaufort Shelf to change in the ice climate

Overall, the phytoplankton productivity values on the Canadian Shelf are characteristic of oligotrophic waters. Values found here for the ice-covered period compare well to those found in the nearshore Alaskan Beaufort Sea (Horner & Schrader 1982, 0.4 g C m^{-2}, April to mid-June). The annual productivities are very similar to those estimated for the nearshore Beaufort Sea by Alexander (1974, 10 to 15 g C m^{-2}) and in the offshore Beaufort by Horner (1981, 10 to 15 g C m^{-2}).

The data presented here suggest that the cycle of phytoplankton productivity on the Canadian Shelf evolves predictably during the season (Fig. 12). In late winter and early spring, there is sufficient nutrient content in the mixed layer to support phytoplankton growth, but the high incident light does not penetrate the water column due to snow and ice cover, resulting in an under-ice system that is essentially light limited. At this time, phytoplankton may begin to grow at the bottom of the ice, ultimately contributing a small (<15%) portion of the annual production (Horner & Schrader 1982) and further shading the water column.

A distinction must be made between domains covered with landfast-ice and pack-ice. Even in the ice-free flaw lead, seaward of the stamukhi, convective mixing driven by brine rejection in late winter acts to deepen the mixed layer to 40 to 50 m, apparently beyond the critical depth so that the overall light climate remains unfavourable for a bloom to occur. The initial load of nutrients at the end of winter is limited by the halocline at the base of the winter mixed layer (represented by a horizontal line in Fig. 12), which restricts the abundant nutrients in the underlying waters of Pacific origin from entering the photic zone. Additional supplies of nutrients, beyond the spring initial load, are thus dependent on forcing by horizontal

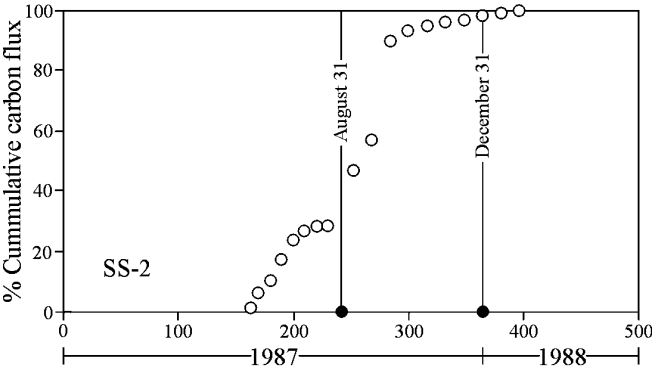

Fig. 11. Vertical flux of carbon at Sediment Trap SS-2 (see Fig. 1 for location). Values on the *x*-axis represent sequential days starting January 1, 1987

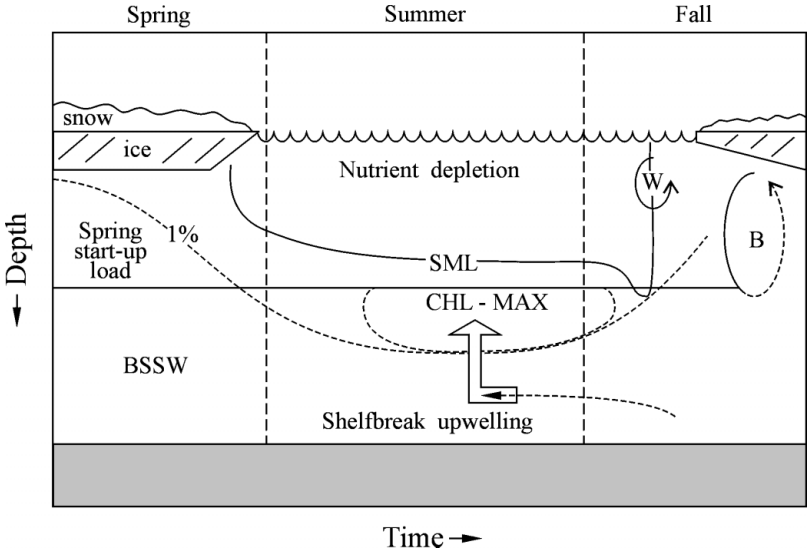

Fig. 12. The annual cycle of pelagic phytoplankton productivity shown schematically as depth versus time. Abbreviations: BSSW = Bering Sea Summer Water; SML = surface mixed layer; W = wind-driven mixing; B = brine-driven mixing by sea-ice formation; CHL-MAX = chlorophyll maximum. The horizontal line across the middle of the diagram depicts the bottom of the winter mixed layer (40 to 50 m) and the dashed line shows the approximate depth where ambient light is 1% of the incident light

(e.g. shelf-break upwelling) or vertical (e.g. turbulent fluxes through the BSSW halocline) processes. According to the scheme shown in Fig. 12, biological productivity on this shelf is ultimately limited by the nutrient supply and not light. Light climate controls the cadence of productivity, allowing initial production at the bottom of the ice and then, as the shelf waters become stratified from ice melt and river inflow, pelagic production in surface water further depletes nutrients. Finally, toward the end of summer, production retreats to a narrow depth range (20 to 50 m) where there is a congruence of stratification, a sufficient supply of nutrients and sufficient light.

Interannual variability in the physical environment of Arctic systems is large and is likely to increase should predictions of global warming prove true (cf. SEARCH SSC 2001). Positive feedback effects (e.g. critical temperatures involving the melting of ice and snow) may amplify the influence of climate warming on Arctic physical systems. Assuming that global warming occurs and that it results in earlier break-up, later freeze-up, thinner ice and a seasonal ice zone that extends farther into the offshore Canada Basin (Serreze et al. 2000, Flato & Boer 2001), the following inferences can be made from the results of the present study. First, an earlier removal of sea-ice cover will certainly affect the timing of the onset of the spring bloom, but the change in light climate is not likely to alter the magnitude of annual production. This is because the spring start-up load of nutrients is set by winter convection, and vertical exchange in summer is limited by the BSSW halocline. A longer exposure of the inner and middle shelf to wind forcing may increase entrainment of nutrients during summer, but will not in itself result in a major alteration in vertical flux. A substantial change would occur, however, should the seasonal ice cover retreat beyond the shelf-break, thus setting critical conditions for the onset of shelf-break upwelling (Carmack & Chapman 2003). Such upwelling would then draw nutrient-rich BSSW into the euphotic zone. Clearly, the duration of time that the shelf-break is ice-free, and the corresponding strength and direction of winds during this time, are critical factors determining the efficiency of upwelling and supply of additional nutrients to the euphotic zone. A delayed freeze-up will also impact productivity but with a delay into the following year. Longer exposure of surface waters to strong winds in winter will both drive low salinity surface waters offshore and bring additional quantities of more saline waters onshore, thus pre-conditioning the shelf with weaker stratification at the onset of freeze-up. Convection driven by brine formation in winter will, thus, be better able to entrain nutrients into the winter mixed-layer by penetrative convection (cf. Melling 1993). In this simple treatment we have assumed that productivity is entirely regulated by so-called bottom-up (light and nutrient regulation) processes, and have ignored surprises that will likely follow from a disturbance to higher predators in the wake of climate variability (see for example Tynan & DeMaster 1997, Hunt & Stabeno 2002).

This brief study leaves great room for improved understanding. Time-series stations should be selected so as to allow better coverage throughout the growing season; especially in the poorly sampled months of mid-June to mid-August. Better measurements of under-ice light climate are needed, especially during early break-up and the Mackenzie River freshet. More information on the vertical distribution of chlorophyll *a* and its temporal variability is required, especially documenting the development and fate of the deep chlorophyll maximum. In this regard, remote sensing is of limited use, in that conditions under sea ice and within the deep chlorophyll maximum are missed, and algorithms currently in use for open waters (surface) cannot separate chlorophyll and suspended sediment signals.

Acknowledgements. We acknowledge the dedicated efforts of F. McLaughlin, M. O'Brien, D. McCullough and L. Cuypers in the collection and analysis of samples. We thank the Polar Continental Shelf Project for providing field accommodation and support during the field work. P. Kimber prepared our figures. The work reported here was funded by the Northern Oil and Gas Action Program (NOGAP) and the Northern Contaminants Program (NCP).

LITERATURE CITED

Aagaard K, Darby D, Falkner K, Flato G, Gerbmeier J, Measures C, Walsh J (1999) Marine science in the Arctic: a strategy. Arctic Research Consortium of the United States (ARCUS), Fairbanks, AK

Alexander V (1974) Primary production regimes of the nearshore Beaufort Sea, with reference to potential roles of ice biota. In: Reed JC, Sater JE (eds) The coast and shelf of the Beaufort Sea. Arctic Inst. North America, Arlington, VA, p 609–632

Anderson LG, Dyrssen D (1981) Chemical constituents of the Arctic Ocean in the Svalbard area. Oceanol Acta 4: 305–311

Carmack EC, Chapman DC (2003) Wind-driven shelf/basin exchange on an Arctic shelf: the joint roles of ice cover extent and shelf-break bathymetry. Geophys Res Lett 30(14):1778

Carmack EC, Kulikov YA (1998) Wind-forced upwelling and internal wave generation in Mackenzie Canyon, Beaufort Sea. J Geophys Res 103:18447–18458

Carmack EC, Macdonald RW (2002) Oceanography of the Canadian Shelf of the Beaufort Sea: a setting for marine life. Arctic 55:29–45

Carmack EC, Macdonald RW, Papadakis JE (1989) Water mass structure and boundaries in the Mackenzie shelf estuary. J Geophys Res 94(C12):18043–18055

Coachman LK, Barnes CA (1961) The contribution of Bering Sea water to the Arctic Ocean. Arctic 14:147–161

Codispoti LA, Richards FA (1968) Micronutrient distributions in the East Siberian and Laptev Seas during summer, 1963. Arctic 21:61–83

Dean KG, Stringer WJ, Ahlnäs K, Searcy C, Weingartner T (1994) The influence of river discharge on the thawing of sea ice, Mackenzie River Delta: albedo and temperature analyses. Polar Res 13:83–94

Fee EJ (1969) A numerical model for the estimation of photosynthetic production, integrated over depth and time, in natural waters. Limnol Oceanogr 14:906–911

Flato GM, Boer GJ (2001) Warming asymmetry in climate change simulations. Geophys Res Lett 28:195–198

Giovando LF, Herlinveaux RH (1981) A discussion of factors influencing dispersion of pollutants in the Beaufort Sea. Report no. 81–4, Institute of Ocean Sciences, Sidney, BC.

Grainger EH (1975) Biological productivity in the southern Beaufort Sea: the physical-chemical environment and the plankton. Beaufort Sea Project Report no. 12a

Harrison PJ, Conway HL, Holmes RW, Davis CO (1977) Marine diatoms grown in chemostats under silicate or ammonium limitation III. Cellular chemical composition and morphology of *Chaetoceros debilis*, *Skeletonema costatum*, and *Thalassiosira gravida*. Mar Biol 43:19–31

Harrison WG, Cota GF (1990) Primary production in polar waters: relation to nutrient availability. Polar Res 10: 87–104

Horner R, Schrader GC (1982) Relative contributions of ice algae, phytoplankton and benthic microalgae to primary production in nearshore regions of the Beaufort Sea. Arctic 35:485–503

Horner RA (1981) Beaufort Sea icebreaker studies. Outer Continental Shelf Environmental Assessment Program (NOAA/MMS), Anchorage AK, Final Report. Biological Studies 13:65–314

Hsiao SIC (1996) Biological productivity of the southern Beaufort Sea: phytoplankton and seaweed studies. Beaufort Sea Technical Report no. 12c, Department of the Environment, Victoria BC

Hunt GL, Stabeno PJ (2002) Climate change and the control of energy flow in the southeastern Bering Sea. Prog Oceanogr 55:5–22

Jasper S, Bothwell ML (1986) Photosynthetic characteristics of lotic periphyton. Can J Fish Aquat Sci 43:1960–1969

Jasper S, Carmack EC, Daley RJ, Gray CBJ, Pharo CH, Wiegand RC (1983) Primary productivity in a large temperate lake with river throughflow: Kootenay Lake, British Columbia. Can J Fish Aquat Sci 40:319–327

Koike I, Ogawa H, Nagata T, Fukuda R, Fukuda H (2001) Silicate to nitrate ratio of the upper sub-arctic Pacific and the Bering Sea Basin in summer: its implication for phytoplankton dynamics. J Oceanogr 57:253–260

Lorenzen CJ (1967) Determination of chlorophyll and pheopigments: spectrophotometric equations. Limnol Oceanogr 12:343–346

Macdonald RW (2000) Arctic estuaries and ice: a positive-negative estuarine couple. In: Lewis EL, Jones EP, Lemke P, Prouse T, Wadhams P (eds) The freshwater budget of the Arctic Ocean. NATO Science series: 2. Environmental security, Vol 70. Kluwer, Dordrecht, p 383–407

Macdonald RW, Carmack EC (1991) The role of large-scale under-ice topography in separating estuary and ocean on an Arctic shelf. Atmos-Ocean 29:37–53

Macdonald RW, Wong CS, Erickson PE (1987) The distribution of nutrients in the southeastern Beaufort Sea: Implications for water circulation and primary production. J Geophys Res 92:2939–2952

Macdonald RW, Iseki K, O'Brien MC, McLaughlin FA and 7 others (1988a) Chemical data collected in the Beaufort Sea and Mackenzie River Delta, Summer, 1987. Can Data Rep Hydrogr Ocean Sci 60(4)

Macdonald RW, Iseki K, O'Brien MC, McLaughlin FA and 6 others (1988b) Chemical data collected in the Beaufort Sea and Mackenzie River Delta, March – July, 1987. Can Data Rep Hydrogr Ocean Sci 60(5)

Macdonald RW, Carmack EC, McLaughlin FA, Iseki K, Macdonald DM, O'Brien MO (1989) Composition and modification of water masses in the Mackenzie Shelf Estuary. J Geophys Res 94:18057–18070

Macdonald RW, Paton DW, Carmack EC, Omstedt A (1995) The freshwater budget and under-ice spreading of Mackenzie River water in the Canadian Beaufort Sea based on salinity and $^{18}O/^{16}O$ measurements in water and ice. J Geophys Res 100:895–919

Macdonald RW, Solomon SM, Cranston RE, Welch HE, Yunker MB, Gobeil C (1998) A sediment and organic carbon budget for the Canadian Beaufort Shelf. Mar Geol 144:255–273

Macdonald RW, Carmack EC, McLaughlin FA, Falkner KK, Swift JH (1999) Connections among ice, runoff and atmospheric forcing in the Beaufort Gyre. Geophys Res Lett 26: 2223–2226

McLaughlin FA, Carmack EC, Macdonald RW, Bishop JKB (1996) Physical and geochemical properties across the Atlantic/Pacific water mass boundary in the southern Canadian Basin. J Geophys Res 101 (C1):1183–1197

McLaughlin FA, Carmack EC, Macdonald RW, Weaver A,

Smith JN (2002) The Canada Basin 1989–1995: Upstream events and far-field effects of the Barents Sea. J Geophys Res 107(C7):10.1029/2001JC000904

McLaughlin FA, Carmack EC, Macdonald RW, Melling H, Swift JH, Wheeler PA, Sherr BF, Sherr EB (2004) The juxtaposition of Atlantic and Pacific-origin waters in the Canada Basin, 1997–1998: A basin in transition. Deep-Sea Res I 51:107–128

Melling H (1993) The formation of a haline shelf front in wintertime in an ice-covered Arctic sea. Cont Shelf Res 13:1123–1147

Melling H, Lewis EL (1982) Shelf drainage flows in the Beaufort Sea and their effect on the Arctic Ocean pycnocline. Deep-Sea Res 29:967–985

Moran SB, Smith JN (2000) ^{234}Th as a tracer of scavenging and particle export in the Beaufort Sea. Cont Shelf Res 20: 153–167

O'Brien MC, Iseki K, Macdonald RW, Forbes JR, Liangfeng Y, McCullough D (1991) Sediment trap data collected in the Beaufort Sea, March 1987–March 1988. Can Data Rep Hydrogr Ocean Sci 60(8)

Omstedt A, Carmack EC, Macdonald RW (1994) Modeling the seasonal cycle of salinity in the Mackenzie shelf/ estuary. J Geophys Res 99:10011–10021

Parsons TR, Webb DG, Dovey H, Haigh R, Lawrence M, Hopky G (1988) Production studies in the Mackenzie River-Beaufort Sea estuary. Polar Biol 8:235–239

Parsons TR, Webb DG, Rokeby BE, Lawrence M, Hopky GE, Chiperzak DB (1989) Autotrophic and heterotrophic production in the Mackenzie River/Beaufort Sea estuary. Polar Biol 9:261–266

Reigstad M, Wassmann P, Riser CW, Øygarden S, Rey F (2002) Variations in hydrography, nutrients and chlorophyll *a* in the marginal ice-zone and the central Barents Sea. J Mar Res 38:9–29

Sakshaug E (2003) Primary and secondary production in the Arctic seas. In: Stein R, Macdonald RW (eds) The organic carbon cycle in the Arctic Ocean. Springer, New York, p 57–81

SEARCH SSC (2001) Study of environmental arctic change. Science Plan, Polar Science Center, Applied Physics Laboratory, University of Washington, Seattle

Serreze MC, Walsh JE, Chapin FSI, Osterkamp T and 6 others (2000) Observational evidence of recent change in the northern high-latitude environment. Clim Change 46: 159–207

Shimada K, Carmack EC, Hatakayama K, Takazawa T (2001) Varieties of shallow temperature maximum waters in the western Canadian Basin of the Arctic Ocean. Geophys Res Lett 28:3441–3444

Tynan C, DeMaster DP (1997) Observations and predictions of Arctic climate change: potential effects on marine mammals. Arctic 50:308–322

Walsh JJ (1989) Arctic carbon sinks: present and future. Global Biogeochem Cycles 3:393–411

Wassmann P (1998) Retention versus export food chains: Processes controlling sinking loss from marine pelagic systems. Hydrobiology 363:29–57

Editorial responsibility: Karl Banse (Contributing Editor), Seattle, Washington, USA

Submitted: October 10, 2003; Accepted: February 7, 2004
Proofs received from author(s): July 21, 2004